The EMBO Journal Vol.17 No.22 pp.6599–6607, 1998

A novel context for the 'MutT' module, a guardian of cell integrity, in a diphosphoinositol polyphosphate phosphohydrolase

Stephen T.Safrany[1], James J.Caffrey, Xiaonian Yang, Michael E.Bembenek[2], Mary B.Moyer[3], William A.Burkhart[3] and Stephen B.Shears

Inositide Signaling Group, National Institute of Environmental Health Sciences, NIH, Research Triangle Park, PO Box 12233, NC 27709, [2]NEN Life Science Products Inc., 549 Albany Street, Boston MA 02118 and [3]Glaxo-Wellcome Research and Development, Department of Analytical Chemistry, Research Triangle Park, NC 27709, USA

[1]Corresponding author
e-mail: safrany@niehs.nih.gov

Diphosphoinositol pentakisphosphate (PP-$InsP_5$ or '$InsP_7$') and bisdiphosphoinositol tetrakisphosphate ($[PP]_2$-$InsP_4$ or '$InsP_8$') are the most highly phosphorylated members of the inositol-based cell signaling family. We have purified a rat hepatic diphosphoinositol polyphosphate phosphohydrolase (DIPP) that cleaves a β-phosphate from the diphosphate groups in PP-$InsP_5$ (K_m = 340 nM) and $[PP]_2$-$InsP_4$ (K_m = 34 nM). Inositol hexakisphophate ($InsP_6$) was not a substrate, but it inhibited metabolism of both $[PP]_2$-$InsP_4$ and PP-$InsP_5$ (IC_{50} = 0.2 and 3 μM, respectively). Microsequencing of DIPP revealed a 'MutT' domain, which in other contexts guards cellular integrity by dephosphorylating 8-oxo-dGTP, which causes AT to CG transversion mutations. The MutT domain also metabolizes some nucleoside phosphates that may play roles in signal transduction. The rat DIPP MutT domain is conserved in a novel recombinant human uterine DIPP. The nucleotide sequence of the human DIPP cDNA was aligned to chromosome 6; the candidate gene contains at least four exons. The dependence of DIPP's catalytic activity upon its MutT domain was confirmed by mutagenesis of a conserved glutamate residue. DIPP's low molecular size, Mg^{2+} dependency and catalytic preference for phosphoanhydride bonds are also features of other MutT-type proteins. Because overlapping substrate specificity is a feature of this class of proteins, our data provide new directions for future studies of higher inositol phosphates.

Keywords: inositol phosphates/MutT/phosphohydrolase

Introduction

The MutT family of proteins are believed to act as homeostatic checkpoints at some important stages in the nucleoside phosphate metabolic pathways, guarding against the potentially dangerous consequences of elevated levels of a small number of these intermediates (Bessman *et al*., 1996; O'Handley *et al*., 1998). The progenitor of this group of enzymes dephosphorylates 8-oxo-dGTP, which promotes high levels of AT to CG transversion mutations (Bhatnagar *et al*., 1991); a *mutT*$^-$ strain of *Escherichia coli* that lacks this catalytic activity has an increased spontaneous mutation rate of up to 10^4-fold (Bessman *et al*., 1996). Mammalian counterparts of this important antimutator dGTPase have been identified (Mo *et al*., 1992). Certain other MutT family members have been proposed to protect the cell from the deleterious consequences of inappropriate activation of some signal transduction processes, by catabolizing additional nucleoside phosphates that may have cell signaling roles (Bessman *et al*., 1996). For example, hydrolysis of dATP by the MutT module (O'Handley *et al*., 1996) may, in mammals, guard against this molecule providing an untimely initiation of apoptosis (Liu *et al*., 1996). Diadenosine polyphosphates, which mediate cellular stress responses (Kisselev *et al*., 1998), are also metabolized by this protein family (Thorne *et al*., 1995). To date, ~15 MutT family members have been characterized, all of which appear dedicated to the metabolism of nucleoside phosphates (Bessman *et al*., 1996). In this report, we describe a novel member of the MutT family that hydrolyzes some metabolically unrelated molecules, namely, diphosphoinositol pentakisphosphate (PP-$InsP_5$ or '$InsP_7$') and bisdiphosphoinositol tetrakisphosphate ($[PP]_2$-$InsP_4$ or '$InsP_8$').

These particular compounds are the most highly phosphorylated representatives of the extended inositol-based family; they were discovered independently by two groups of researchers in 1993 (Menniti *et al*., 1993; Stephens *et al*., 1993). PP-$InsP_5$ and $[PP]_2$-$InsP_4$ occur in many different cell types from across the phylogenetic spectrum (Martin *et al*., 1993, 1995; Menniti *et al*., 1993; Stephens *et al*., 1993; Albert *et al*., 1997). The metabolism of the diphosphorylated inositol polyphosphates is intertwined with some intriguing signal transduction processes. For example, PP-$InsP_5$ turnover in intact cells is perturbed upon Ca^{2+} pool depletion by thapsigargin, a tumor promoter (Glennon and Shears, 1993). Interest in the mechanisms of the latter phenomenon reflects current concern over the nature of cytosolic effectors that can sense changes in the Ca^{2+} concentration of the endoplasmic reticulum (Putney, 1991). Moreover, it was shown recently that $[PP]_2$-$InsP_4$ metabolism is regulated by β-adrenergic agonists; this response was downstream of cAMP, but unusual in nature because it was independent of the activation of either protein kinase A (PKA) or PKG (Safrany and Shears, 1998).

PP-$InsP_5$ and $[PP]_2$-$InsP_4$ are formed from the cell's metabolic reservoir of $InsP_6$ (Menniti *et al*., 1993; Stephens *et al*., 1993). An ATP-dependent $InsP_6$ kinase synthesizes PP-$InsP_5$ (Voglmaier *et al*., 1996); an ATP-dependent PP-$InsP_5$ kinase produces $[PP]_2$-$InsP_4$ (Shears *et al*., 1995; Voglmaier *et al*., 1997). PP-$InsP_5$ and $[PP]_2$-$InsP_4$ are both

Table I. Purification of DIPP

Step	Protein (μg)	Substrate	Specific activity (k^{-1}/μg/min)	Total activity (k^{-1}/min)	Purification (-fold)	Yield (%)
Homogenate	17 000 000	PP-$InsP_5$	0.00038	6500	1	100
		$[PP]_2$-$InsP_4$	0.00013	2200	1	100
Supernatant	14 000 000	PP-$InsP_5$	0.00036	5000	0.95	77
		$[PP]_2$-$InsP_4$	0.00010	1400	0.77	64
Polyethylene glycol	3 300 000	PP-$InsP_5$	0.00067	2200	1.8	34
		$[PP]_2$-$InsP_4$	0.00029	960	2.2	44
Mono Q	150 000	PP-$InsP_5$	0.010	1500	27	23
		$[PP]_2$-$InsP_4$	0.0046	690	35	31
Heparin–agarose	440	PP-$InsP_5$	0.81	360	2100	5.5
		$[PP]_2$-$InsP_4$	0.15	66	1200	3.0
Green A	16	PP-$InsP_5$	4.2	67	11 000	1.0
		$[PP]_2$-$InsP_4$	1.3	21	10 000	0.95
Cellufine/Blue A	0.19	PP-$InsP_5$	50	9.5	130 000	0.15
		$[PP]_2$-$InsP_4$	17	3.2	130 000	0.15

To estimate enzyme activities, the integrated first-order rate equation, $[S] = [S]_0e^{-kt}$ was used to calculate a first-order rate constant (k^{-1}).

dephosphorylated rapidly back to $InsP_6$, both *in vivo* and upon their addition to cell homogenates (Shears *et al*., 1995), but there is no previously published information concerning the nature of the enzymes that are responsible for these reactions. In this study, we describe for the first time the detailed biochemical and molecular characterization of a phosphohydrolase that metabolizes both of these diphosphorylated polyphosphates. We have therefore named this novel enzyme a diphosphoinositol polyphosphate phosphohydrolase ('DIPP'). A particularly exciting aspect of this study is our discovery that the catalytic activity of this protein uses a MutT domain in a novel context.

Results

Purification of DIPP from rat liver

When PP-$InsP_5$ and $[PP]_2$-$InsP_4$ are added to cell homogenates, they are both dephosphorylated rapidly to $InsP_6$ (Menniti *et al*., 1993; Shears *et al*., 1995). These phosphohydrolase activities, which predominated in a 100 000 *g* soluble fraction, were concentrated ~2-fold by precipitating other proteins from the cytosol using 22% (w/v) polyethylene glycol (Table I). The supernatant was then fractionated further by Mono Q anion-exchange chromatography. A major peak of phosphohydrolase activity was eluted with ~200 mM NaCl. This enzyme activity was purified further by heparin–agarose affinity chromatography and Green A dye–ligand chromatography; in each case, a peak of enzyme activity was eluted with ~500 mM NaCl. The low molecular weight of the enzyme (~20 kDa, see below) facilitated its further purification by gel filtration, following which the enzyme was purified further by Blue A affinity chromatography. The final preparations of enzyme, which we have named DIPP in this report (see Introduction), were purified ~130 000-fold with a 0.15% yield (Table I). Note that DIPP activity against PP-$InsP_5$ and $[PP]_2$-$InsP_4$ co-purified (Table I).

Characterization of DIPP

DIPP activity was $[Mg^{2+}]$ dependent; 1–2 mM was required for maximal activity (Figure 1A). Gel filtration (Figure 1B) indicated that the apparent molecular size of DIPP was 18 ± 1.5 kDa ($n = 3$). An identical result was obtained under thiol reducing conditions with 1 mM dithiothreitol (DTT) added, indicating that DIPP is a monomer. The K_m for $[PP]_2$-$InsP_4$ (Figure 1C) was 34 ± 7 nM ($n = 7$). The affinity for PP-$InsP_5$ (Figure 1D) was 10-fold lower (K_m = 340 ± 50 nM, $n = 9$). These K_m values are very close to the cellular levels of these metabolites (Shears *et al*., 1995), suggesting that their rate of metabolism by DIPP *in vivo* will be dependent upon substrate supply. The V_{max} for PP-$InsP_5$ was 330 ± 99 nmol/mg protein/min ($n = 8$), whereas the V_{max} for $[PP]_2$-$InsP_4$ was 9-fold lower (37 ± 6 nmol/mg protein/min, $n = 7$). DIPP was very specific for diphosphoinositol polyphosphates; $InsP_6$, Ins(1,3,4,5,6)P_5, Ins(1,2,4,5,6)P_5 and Ins(1,3,4,5)P_4 were not hydrolyzed (not shown). It was also notable that upon incubation of DIPP with ADP and either [5-β-^{32}P]PP-$InsP_5$ or 5-PP-[6-β-^{32}P]PP-$InsP_4$, all of the ^{32}P that was hydrolyzed was recovered as [^{32}P]P_i (data not shown). That is, DIPP does not act as an ATP synthase, in contrast to the 'reverse' activities of the $InsP_6$ kinase (Voglmaier *et al*., 1996).

Fluoride (F^-) was a potent inhibitor of DIPP activity against both $[PP]_2$-$InsP_4$ (K_i = 8.4 ± 0.4 μM, $n = 3$) and PP-$InsP_5$ (K_i = 10.9 ± 0.6 μM, $n = 4$) (Figure 1E and F). Possibly related to the fact that the diphosphate group on $[PP]_2$-$InsP_4$ that is attacked is different from the diphosphate on PP-$InsP_5$ that is hydrolyzed (Shears *et al*., 1995), there was an important difference in the mechanism by which F^- inhibited these two reactions. In the case of the PP-$InsP_5$ phosphatase activity, F^- was a non-competitive inhibitor (Figure 1F). In contrast, F^- inhibited $[PP]_2$-$InsP_4$ phosphatase activity in an uncompetitive manner (Figure 1E). This observation is not unprecedented; inhibition of inositol monophosphatase by F^- is competitive against glycerol-2-phosphate as substrate, but non-competitive against Ins1P as substrate (Ganzhorn and Chanal, 1990).

Regulation of DIPP

$InsP_6$ is not a substrate of DIPP (see above), but it inhibited the dephosphorylation of both PP-$InsP_5$ and $[PP]_2$-$InsP_4$; average IC_{50} values for $InsP_6$ were 3 and 0.2 μM ($n = 4$), respectively, when DIPP was incubated with physiologically relevant concentrations of PP-$InsP_5$ (200 nM) and $[PP]_2$-$InsP_4$ (40 nM). This inhibition is likely to be significant *in vivo*, since liver contains ~10 μM $InsP_6$

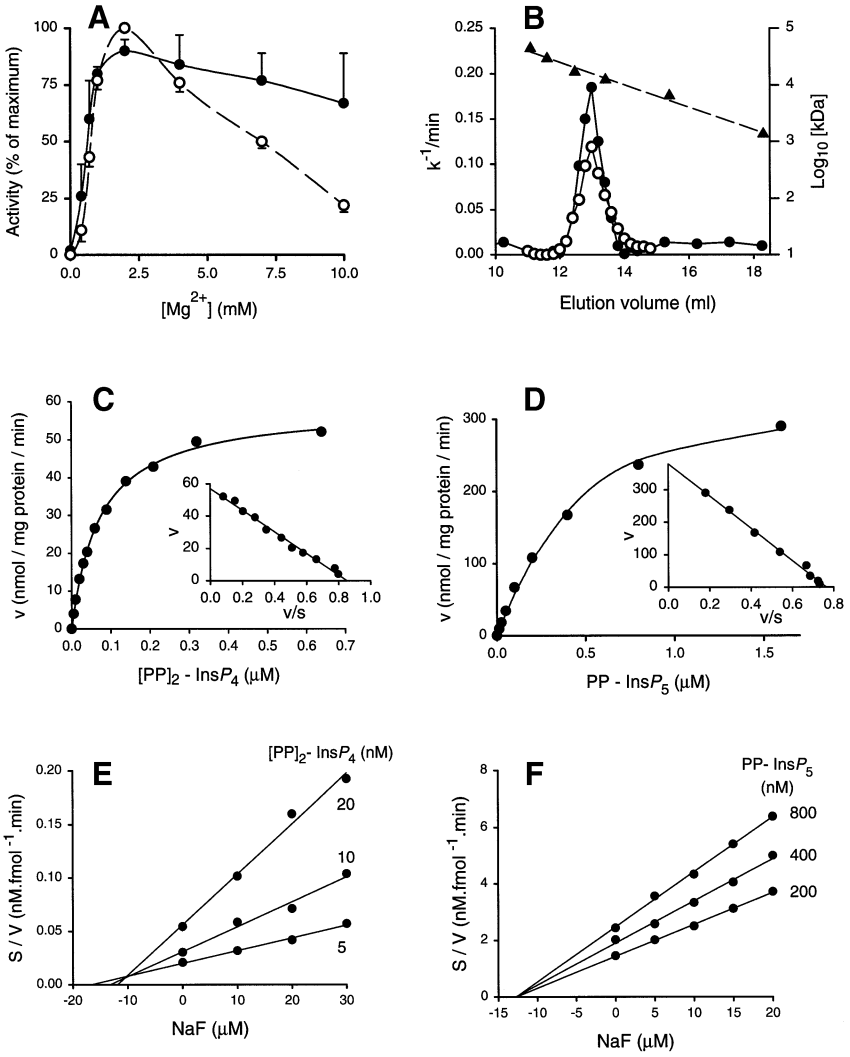

Fig. 1. Properties of purified DIPP. (**A**) $[Mg^{2+}]$ dependence of DIPP activity against PP-$InsP_5$ (●) and $[PP]_2$-$InsP_4$ (○). (**B**) PP-$InsP_5$ phosphatase (●) and $[PP]_2$-$InsP_4$ phosphatase (○) activities were chromatographed on Superdex 75 HR 10/30 resin (Pharmacia Biotechnology, Piscataway, NJ) equilibrated with 10 mM Bis-Tris, 250 mM NaCl (pH 7.2 with HCl). The protein was eluted at a flow rate of 0.2 ml/min, and 250 μl fractions were collected and assayed. The following molecular weight markers were used (Bio-Rad and Sigma) (▲): aprotinin (6.5 kDa), cytochrome *c* (12.4 kDa), carbonic anhydrase (29 kDa), vitamin B_{12} (1.35 kDa), equine myoglobin (17 kDa) and chicken ovalbumin (44 kDa). (**C**) Kinetics of $[PP]_2$-$InsP_4$ hydrolysis. (**D**) Kinetics of PP-$InsP_5$ hydrolysis. (**E**) Inhibition of $[PP]_2$-$InsP_4$ hydrolysis by F^-. (**F**) Inhibition of PP-$InsP_5$ hydrolysis by F^-.

(Szwergold *et al*., 1987). The 2-phosphate of $InsP_6$ makes a contribution to the specificity of inhibition, since Ins(1,3,4,5,6)P_5 was an 8-fold weaker inhibitor (the IC_{50} values were 25 μM against PP-$InsP_5$ as substrate, and 1.6 μM with $[PP]_2$-$InsP_4$ as substrate, $n = 4$). Ins(1,3,4,5)P_4 and Ins(1,4,5)P_3 were considerably weaker inhibitors [IC_{50} values were >100 μM, which is well in excess of their physiological levels; Shears (1992)].

We have shown previously that, in intact cells, cAMP caused levels of $[PP]_2$-$InsP_4$ to decrease in a PKA-independent manner (Safrany and Shears, 1998). It was therefore an important confirmatory observation that PKA had no effect upon DIPP-mediated hydrolysis of either $[PP]_2$-$InsP_4$ or PP-$InsP_5$ (data not shown; see Materials and methods for details). By itself, cAMP (from 0.01 to 10 mM) also had no effect upon DIPP activity (data not shown). DIPP was also unaffected upon its reconstitution with PKC (data not shown; see Materials and methods for details), or by elevating free $[Ca^{2+}]$ from 0.1 to 1 μM (both in the presence and absence of calmodulin; data not shown).

Molecular cloning, expression and site-directed mutagenesis of human DIPP

A considerable proportion of native rat DIPP was microsequenced (Figure 2A). Database searching with the BLAST algorithm revealed a close match between this microsequence and the predicted amino acid sequence encoded by an expressed sequence tag (EST) cDNA (DDBJ/EMBL/GenBank accession No. AA043224), which contains a 1222 bp cDNA insert isolated from human adult uterus. We sequenced this clone and found that an open reading frame from nucleotides 154 to 669 encodes the predicted 172 amino acid sequence depicted in Figure 2A; the predicted mol. wt is 19.5 kDa, which is close to our determination of the size of the native rat protein. The predicted amino acid sequence of the human protein aligns exactly with the microsequence of the native rat enzyme (excluding four residues in the rat microsequence that could not be identified independently; Figure 2A).

The DIPP cDNA has a candidate initiator codon within a weak Kozak consensus (Kozak, 1996), upstream of

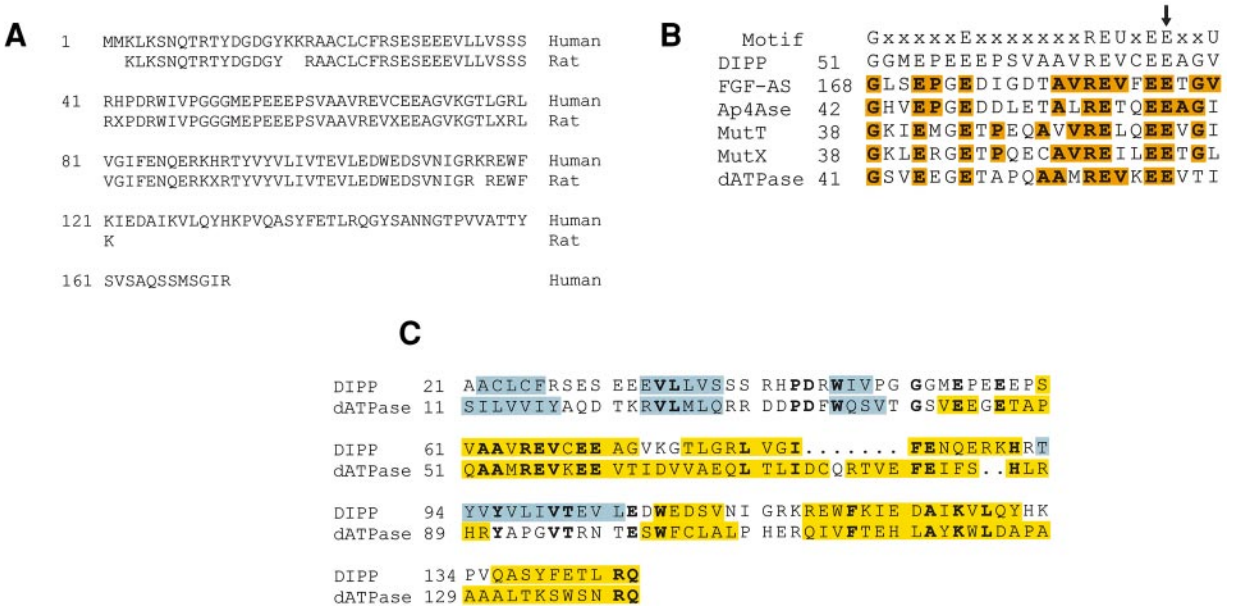

Fig. 2. Amino acid sequence of rat and human DIPP. (**A**) The partial sequence of rat DIPP was obtained from Lys-C and CNBr digests; 'X' indicates amino acid residues that could not be identified independently. This sequence was aligned with the predicted amino acid sequence of human DIPP (DDBJ/EMBL/GenBank accession No. AF062529). (**B**) The MutT domain ('x' represents any amino acid, and 'U' indicates either of the bulky aliphatic amino acids, I, L or V) from human DIPP is aligned with corresponding regions from the protein product of the antisense transcript of rat fibroblast growth factor (P70563), human diadenosine tetraphosphate hydrolase (U30313), MutX from *Streptococcus pneumoniae* (S41532), MutT from *E.coli* (P08337) and *orf17* dATPase from *E.coli* (P24236). Residues identical to those in DIPP are highlighted in orange. A catalytically essential Glu residue (Lin *et al*., 1996) is marked with an arrow. (**C**) Amino acid sequence alignment of the central cores of human DIPP and dATPase from *E.coli* (P24236). Identical residues are in bold type. Secondary structure (as predicted by a 'consensus' method using Peptool v1, Natural Biosciences Inc., Plymouth, MN) is highlighted in either blue (for β-sheets) or yellow (for α-helices).

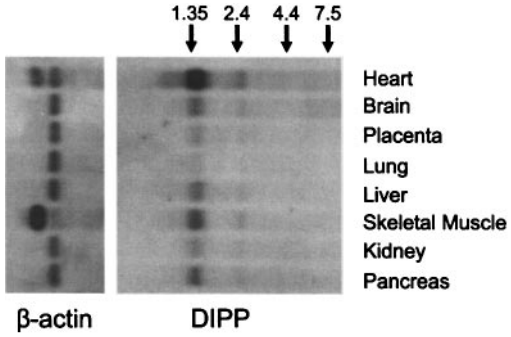

Fig. 3. Northern blot analysis of human mRNA. A Northern blot containing poly(A)-selected RNA from various human tissues (nominally 2 μg/lane) was probed using a DIPP cDNA probe as described in Materials and methods. The relative intensities of each of the signals were as follows (determined using an imaging densitometer, and expressed as a ratio to the corresponding β-actin controls): brain = 1.1, pancreas = 0.9, heart and liver = 0.8, placenta and kidney = 0.5, skeletal muscle and lung = 0.3. Two additional blots gave similar results.

which are 153 nucleotides that are exceptionally G/C rich (80%), and do not contain an in-frame start or stop codon; these are characteristics of 5′ non-translated nucleotide sequences that regulate the expression of cell signaling proteins of particularly low abundance (Kozak, 1996). There is an 18 nucleotide poly(A) tail at the 3′ terminus of the clone, beginning 14 nucleotides downstream of a candidate polyadenylation signal. Northern blots (Figure 3) revealed that a 1.4 kb DIPP mRNA was present in a range of human tissues, with the mRNA signal being expressed most prominently in brain, heart, pancreas and liver (after compensating for differing expression of β-actin mRNA, see legend to Figure 3). A BLAST search indicated that much of the DIPP cDNA aligned with discrete regions of the DNA sequence of chromosome 6 (6p21.2–6p21.33, Figure 4). This is likely to be where the gene for DIPP is located, within which we have identified four candidate exons (Figure 4), each of which obeys the GT–AG splice site rule (Jackson, 1991).

Escherichia coli was used as an expression system for a His-tagged form of DIPP that was then purified, in a single step, to apparent homogeneity (Figure 5A, lane 1). Note that the protein migrates with an approximate mol. wt of 25 kDa upon SDS–PAGE. This recombinant protein was found to hydrolyze both $[PP]_2$-$InsP_4$ and PP-$InsP_5$ (Figure 5B and C). The specific activity of recombinant human DIPP (2500 ± 500 and 380 ± 37 k^{-1}/μg/min for PP-$InsP_5$ and $[PP]_2$-$InsP_4$, respectively, $n = 4$) was 20- to 50-fold greater than the specific activity of purified native rat DIPP (Table I), which may be explained by the instability of the latter enzyme during the long purification procedure. The determination that DIPP dephosphorylates both $[PP]_2$-$InsP_4$ and PP-$InsP_5$ was an unexpected result since the positional specificity of the phosphohydrolase is different for each substrate. In PP-$InsP_5$, the diphosphate group that is attached to the 5-carbon is hydrolyzed (Shears *et al*., 1995; Albert *et al*., 1997). The 5-diphosphate is also present in $[PP]_2$-$InsP_4$, but it is the other diphosphate group in this compound which is attacked specifically (Shears *et al*., 1995). It has, therefore, been anticipated that a single enzyme would not have the required differential specificity towards these two substrates (Shears *et al*., 1995).

A prominent feature of the amino acid sequence of DIPP is that it contains a MutT module (Figure 2A and B). The similarity of DIPP's MutT domain to several

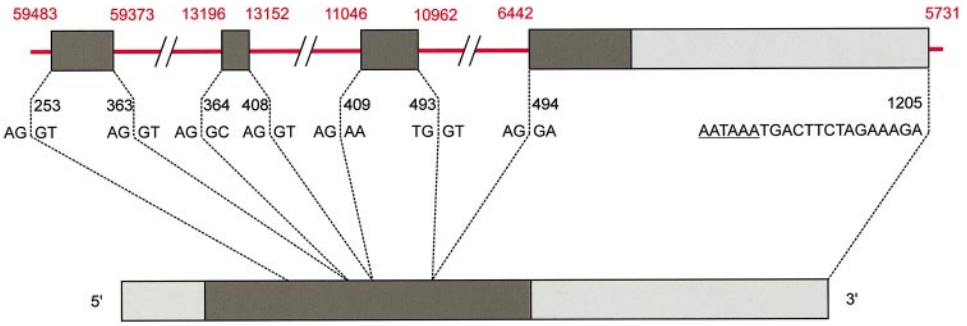

Fig. 4. Schematic alignment of DIPP cDNA with PAC187N21 human DNA. The human DIPP mRNA sequence (dark gray = translated, light gray = non-translated) was aligned with the human genomic DNA sequence from the PAC187N21 contig (DDBJ/EMBL/GenBank accession No. Z98036) on chromosome 6p21.2–6p21.33 (red line). The most 5′ and 3′ nucleotides of each predicted exon are numbered (red = genomic DNA sequence, black = DIPP cDNA). The identity of the two nucleotides either side of each predicted intron–exon boundary is also indicated. The 21 nucleotide 3′ terminus of the DIPP cDNA is also given, so as to show the position of the polyadenylation signal (underlined).

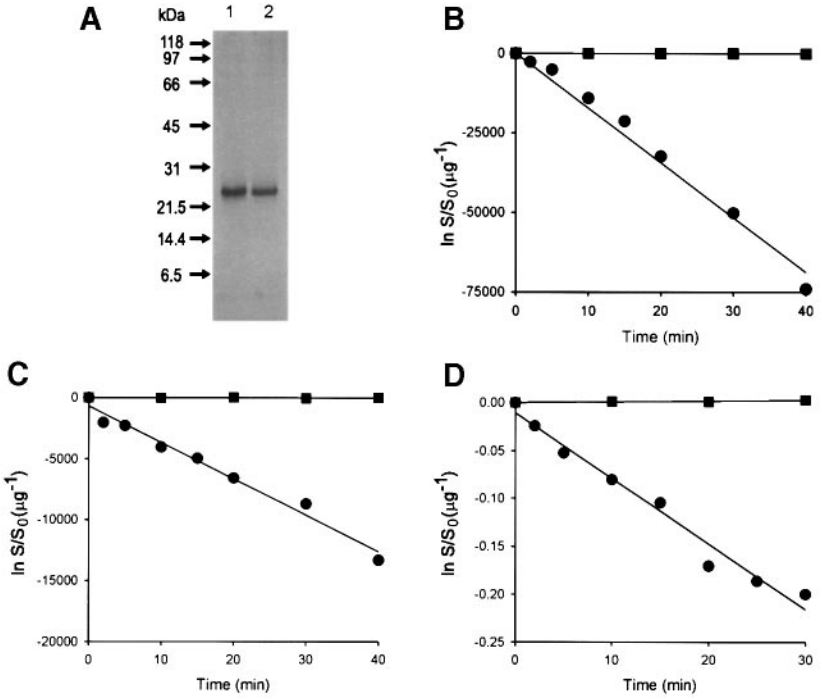

Fig. 5. Expression and catalytic activity of recombinant DIPP. Wild-type (**A**, lane 1) and an E70Q mutant (A, lane 2) His-tagged DIPP were expressed in *E.coli* and purified (see Materials and methods). Purity was determined by silver staining a 4–12% Bis-Tris NuPage gel (Novex, CA), run with MES buffer according to the manufacturer's instructions using 10 μg of DIPP. The molecular weight markers (from bottom to top) were: aprotinin, lysozyme, trypsin inhibitor, carbonic anhydrase, ovalbumin, serum albumin, phosphorylase B and β-galactosidase. Catalytic activities of the wild-type DIPP (●) and the E70Q mutant (■) were determined against the following substrates: PP-$InsP_5$ (**B**), $[PP]_2$-$InsP_4$ (**C**) or dATP (**D**). For inositol phosphate hydrolysis, each data point represents the results of an individual HPLC analysis. dATPase assays were determined in duplicate (mean range ± 7%). The first-order rate constants (μg^{-1}/min) were obtained by regression analysis of all the data points. Data shown are from a representative experiment. The mean rate constants (± SE) from four preparations of wild-type DIPP were as follows: PP-$InsP_5$ = 2500 ± 500; $[PP]_2$-$InsP_4$ = 380 ± 37; dATP = 0.008 ± 0.001. None of the three preparations of E70Q mutants expressed any significant activity.

other examples of this motif goes beyond the eight signature amino acids of the 23 residue module; the degree of identity ranges from 43 to 57% (Figure 2B). Furthermore, the MutT domain assumes an α-helical structure (Lin *et al*., 1996), and this is also predicted to be conserved in DIPP (Figure 2C). The occurrence of a MutT consensus sequence in an enzyme responsible for metabolizing inositol polyphosphates was unexpected, since this domain previously has been designated as imparting catalytic specificity solely towards nucleoside phosphates (Bessman *et al*., 1996).

The primary sequence that lies either side of the MutT domain in DIPP aligned only poorly with corresponding regions of the other MutT family members listed in Figure 2B (the GAP algorithm estimated that the percentage identities ranged from 14 to 22%). The various MutT family members also show little overall conservation of primary sequence (Bessman *et al*., 1996). However, it is possible that these regions that are external to the MutT domain may sometimes share some similarities in secondary structure, such as is predicted to be the case with DIPP and a MutT-type dATP pyrophosphohydrolase (dATPase), a product of the *orf17* gene of *E.coli* (O'Handley *et al*., 1996) (Figure 2C). Nevertheless, dATP is not likely to be a physiologically relevant substrate of DIPP; although dATP can be dephosphorylated by this

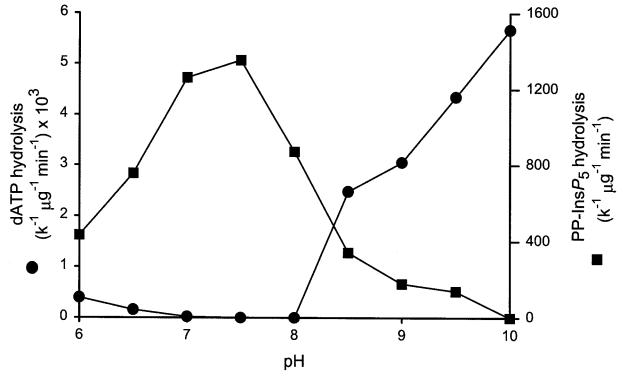

Fig. 6. pH optima of recombinant DIPP. Recombinant DIPP activity against PP-InsP$_5$ (■) or dATP (●) was assayed as described in Materials and methods except that the buffering system comprised 12 mM Bis-Tris, 12 mM HEPES, 12 mM Tris and 12 mM CAPSO, adjusted to the indicated pH with KOH and HCl. For inositol phosphate hydrolysis, each data point represents the results of an individual HPLC analysis. dATPase assays were determined in duplicate (mean range ± 7%). Data are from a representative experiment, typical of either three (for PP-InsP$_5$) or six (for dATP).

enzyme *in vitro*, the rate constant for this reaction was several orders of magnitude less than that for either PP-InsP$_5$ or [PP]$_2$-InsP$_4$ (Figure 5). The pH optimum for dATP also exceeded a value of 9 (Figure 6). As it happens, an alkaline pH optimum is rather typical of the MutT class of enzymes (O'Handley *et al*., 1996, 1998). In contrast, PP-InsP$_5$ hydrolysis by DIPP had a pH optimum of 7.0–7.5 (Figure 6).

Conserved glutamate residues within the MutT domain are believed to participate in both binding of the Mg^{2+}–substrate complex and in general base catalysis (Lin *et al*., 1996, 1997). The introduction of an E57Q mutation within a prototypical MutT domain, namely an *E.coli* dGTP pyrophosphohydrolase (see Figure 2B), has been shown previously to reduce its catalytic activity 10^5-fold (Lin *et al*., 1996). This Glu57 residue aligned with Glu70 in the MutT domain of DIPP (Figure 2B). We therefore generated an E70Q mutant of DIPP by site-directed mutagenesis. This protein was expressed in *E.coli* (Figure 5A, lane 2) at levels comparable with that of the wild-type protein (Figure 5A, lane 1). The E70Q mutant was found to be essentially inactive against either dATP, PP-InsP$_5$ or [PP]$_2$-InsP$_4$ (Figure 5). This result demonstrates that the MutT domain of DIPP participates in the hydrolysis of all three substrates. This result is of particular importance because it will lead us to revise an earlier idea that the MutT signature designates a unique binding domain for nucleoside phosphates (O'Handley *et al*., 1996).

Phosphohydrolase activity of DIPP

In view of the fact that DIPP brings a new genre of substrate specificity to the MutT family, it was particularly important to assess the reaction products. Our assays demonstrated that DIPP expressed phosphohydrolase activity against both PP-InsP$_5$ and [PP]$_2$-InsP$_4$, i.e. Pi was released (see Materials and methods). Furthermore, when these assays of DIPP activity were supplemented with inorganic pyrophosphatase (which converts PPi to 2Pi), there was no increase in the total Pi signal (data not shown). Thus, DIPP does not release PPi from its substrates. This conclusion was confirmed further by HPLC analysis (Figure 7A). Here, PP-[^{3}H]InsP$_5$ was shown to be dephosphorylated to [^{3}H]InsP$_6$ (i.e. by removal of the β-phosphate in the diphosphate group). In these experiments, there was no accumulation of InsP$_5$ (which would have been formed if the diphosphate group were removed from PP-InsP$_5$), nor was any PP-InsP$_4$ detected (which would have reflected cleavage of a monoesterphosphate from PP-InsP$_5$). Thus, DIPP obeys another general paradigm of MutT activity, namely hydrolysis of a phosphoanhydride linkage (Bessman *et al*., 1996). We also investigated the products of dATP hydrolysis. Figure 7B clearly demonstrates that Pi was released from dATP, yielding dADP. This result contrasts starkly with other MutT-type proteins, which release PPi from nucleoside triphosphates (O'Handley *et al*., 1996).

Discussion

Prior to this study, almost nothing was known of the nature of the enzymes that dephosphorylate PP-InsP$_5$ and [PP]$_2$-InsP$_4$ *in vivo*. Therefore, we have added considerably to our knowledge of this subject with the purification, characterization and sequencing of a cDNA clone of an enzyme, DIPP, that actively metabolizes both of these diphosphorylated substrates.

Our study raises the possibility that, *in vivo*, diphosphorylated inositol polyphosphates and nucleoside phosphates may compete for the active sites of some MutT-type proteins. Indeed, overlapping catalytic specificities, at least towards the various nucleoside phosphate substrates, has already proved to be a feature of individual members of the MutT family (O'Handley *et al*., 1998). This has considerable implications for further studies into the functions of both the diphosphorylated inositides and the nucleoside phosphates. To take one example, if PP-InsP$_5$ and [PP]$_2$-InsP$_4$ competed with dATP for a MutT catalytic site *in vivo*, this could impact upon the role of dATP metabolism in regulating apoptosis (Liu *et al*., 1996). This will be an important area for future research, as >100 nucleotide sequences that potentially code for MutT proteins are now known; only ~15 of these have defined protein products (Bessman *et al*., 1996; O'Handley *et al*., 1998). Further studies along these lines should take into account that the hydrolysis of diphosphoinositol polyphosphates by DIPP is optimal under physiologically relevant conditions of a near neutral pH (Figure 6) and a [Mg^{2+}] of 1–2 mM (Figure 1A). In contrast, the metabolism of nucleoside phosphates by most MutT-type enzymes is optimal when [Mg^{2+}] = 8–10 mM and the pH is 8.5–9.0 (Bhatnagar *et al*., 1991; Bullions *et al*., 1994; O'Handley *et al*., 1996). Thus, if other MutT-type proteins do metabolize PP-InsP$_5$ and [PP]$_2$-InsP$_4$, it is reasonable to anticipate that these reactions could be favored by the intracellular environment, at the expense of the hydrolysis of nucleoside phosphates.

InsP$_6$ was not a substrate of DIPP, but it clearly can bind to this enzyme and inhibit its activity, particularly against [PP]$_2$-InsP$_4$ as substrate (IC_{50} = 0.2 μM, see Results). Several studies reveal circumstances under which DIPP activity *in vivo* could be regulated by alterations in cellular levels of InsP$_6$. For example, there is evidence that the size of at least one of the cellular InsP$_6$ pools may be acutely sensitive to receptor activation (Singh

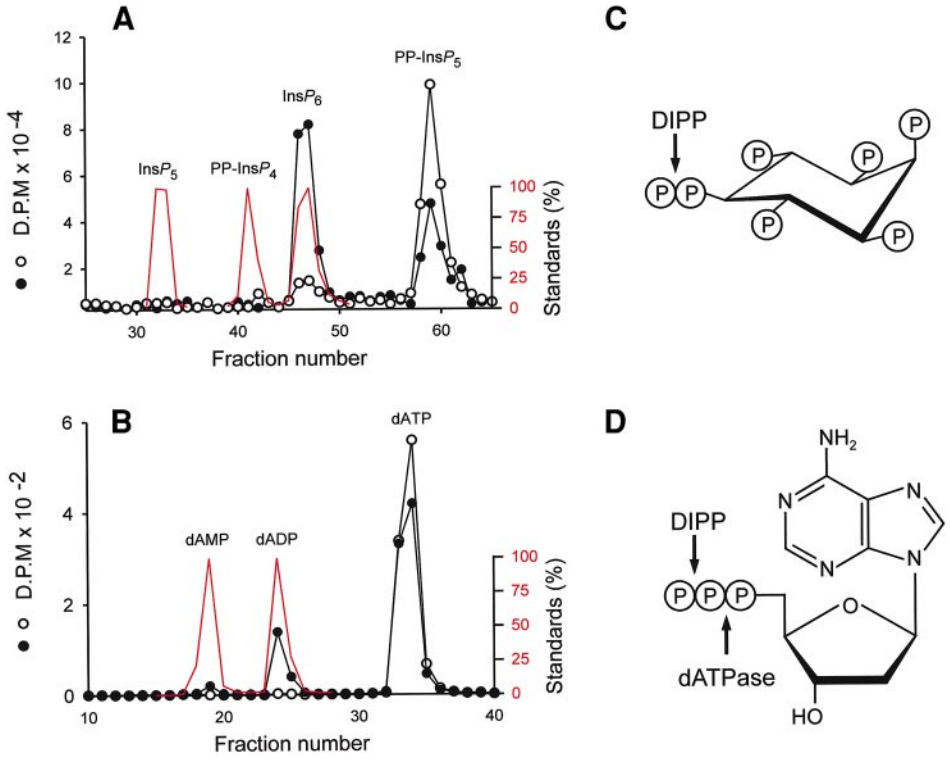

Fig. 7. HPLC analysis of DIPP-mediated hydrolysis of PP-InsP_5 and dATP. DIPP activity towards [^{3}H]PP-InsP_5 (**A**) or [^{3}H]dATP (**B**) was assayed and analyzed by HPLC as described in Materials and methods (●). Data shown are a representative example of three experiments. The corresponding HPLC profile from a zero time control is also shown (○). The elution positions of standards are shown in red (plotted as a percentage of maximum peak height). In (A), the elution of the standards was determined in adjacent HPLC runs. In (B), the eluate A_{260} was monitored to determine the elution of non-radiolabeled internal standards. The structures of PP-InsP_5 (**C**) and dATP (**D**), and the differing hydrolytic specificites of DIPP and the *E.coli* MutT-type dATPase (O'Handley *et al*., 1996) are also indicated.

et al., 1996). Some rather substantial changes in total cellular InsP_6 levels have also been noted during cell differentiation (French *et al*., 1991). Finally, a dramatic up-regulation of cellular InsP_6 phosphatase activity precedes chondrocyte cell death during the bone ossification process (Craxton *et al*., 1997; Romano *et al*., 1998). Changes in cellular InsP_6 levels may not only regulate the activity of DIPP, but may also affect other MutT-type activities.

It has been argued that the MutT motif is primordial in origin (Bessman *et al*., 1996). DIPP, too, is most likely to have arisen at an early evolutionary stage, because the ability to synthesize and metabolize the diphosphorylated inositol polyphosphate is widely distributed throughout nature, from mammals (Shears *et al*., 1995; this study), through yeast (Ali *et al*., 1995), slime molds (Stephens *et al*., 1993), plants (Brearley and Hanke, 1996) and microorganisms such as *Phreatamoeba balamuthi* (Martin *et al*., 1995) and *Entamoeba histolytica* (Martin *et al*., 1993). There is considerable conservation of primary sequence between the rat and human forms of DIPP (Figure 2A). It will be interesting to determine the extent to which DIPP, and the functions of PP-InsP_5 and [PP]$_2$-InsP_4, are conserved across the phylogenetic spectrum.

Materials and methods

Assay of DIPP

DIPP activity against PP-InsP_5 and [PP]$_2$-InsP_4 was determined routinely at 37°C in 500 µl of medium containing 50 mM KCl, 50 mM HEPES (pH 7.2 with KOH), 4 mM CHAPS, 0.05 mg/ml bovine serum albumin (BSA), 1 mM Na_2EDTA, 2 mM $MgSO_4$. The reactions were quenched by the addition of ice-cold 8% perchloric acid (500 µl) containing 1 mg/ml InsP_6, and then neutralized as previously described (Safrany and Shears, 1998). In some experiments, release of Pi was recorded using an assay (Hoenig *et al*., 1989) that does not detect PPi. Elsewhere, the metabolism of ^{3}H-labeled substrates was assayed by HPLC (Safrany and Shears, 1998), or we used gravity-fed ion-exchange columns (Shears *et al*., 1995) to measure [^{32}P]P_i release from either [5-β-^{32}P]PP-InsP_5 or 5-PP-[6-β-^{32}P]PP-InsP_4 [note that the second diphosphate group is only tentatively assigned to the 6-carbon; Safrany and Shears (1998)].

In some experiments, DIPP activity was assayed in the presence of 10 µM calmodulin (Calbiochem), whereupon $[Ca^{2+}]_{free}$ was adjusted from 0.1 µM to 1 µM. DIPP was also assayed after pre-incubation for 5 min with either (i) 100 U of the catalytic subunit of PKA (Pierce) plus 2 mM ATP and 10 mM $MgCl_2$ (in parallel incubations where 11 µg of dye-labeled Kemptide substrate was added instead of DIPP, >80% of the substrate was phosphorylated) or (ii) 0.1 U of PKC (Pierce) plus 100 nM phorbol 12-myristate 13-acetate, 200 µg/ml phosphatidyl-L-serine, 2 mM ATP, 10 mM $MgCl_2$ and 0.1 mM $CaCl_2$ (in parallel incubations where 16 µg of dye-labeled glycogen synthase peptide substrate was added instead of DIPP, >80% of the substrate was phosphorylated).

DIPP activity towards [^{3}H]dATP was assayed routinely in buffer containing 50 mM Tris (pH 9.0 with HCl), 10 mM $MgSO_4$, 1 mM DTT, 0.05 mg/ml BSA (O'Handley *et al*., 1996). Samples were quenched either with ice-cold water (for HPLC analysis) or 0.2 M ammonium formate/0.1 M formic acid for assay by gravity-fed anion-exchange ('Dowex') columns. HPLC was performed using a 4.6×125 mm Partisphere 5 µm SAX column. Samples were eluted at 1 ml/min by the following gradient generated by mixing buffer A (1 mM Na_2EDTA) with buffer B [1.3M $(NH_4)_2HPO_4$, pH 3.85 with H_3PO_4, plus 1 mM Na_2EDTA]: 0–1 min, 0% buffer B; 1–30 min, 0–30% buffer B; 31–36 min, 100% buffer B.

Purification of DIPP

Frozen rat livers (50 g) (Pel-Freeze Biologicals, Rogers, AR) were allowed to thaw at 4°C, homogenized, and a 100 000 *g* supernatant was prepared as previously described (Shears *et al*., 1995). A 22% (w/v)

polyethylene glycol 4000 (Fluka) precipitate was then removed by centrifugation. The supernatant was diluted 2:1 (v/v) with 10 mM triethanolamine (pH 8.0 with NaOH) (buffer A), and DIPP was purified by the following steps.

Column 1, Mono-Q HR, 16 mm×10 cm (Pharmacia LKB Biotechnology Inc., Piscataway, NJ) (flow-rate = 1 ml/min). After sample loading, the column was eluted with a gradient generated by mixing buffer A with buffer B (buffer A plus 1 M NaCl): 0–90 min, 0% buffer B; 90–290 min, 0–25% buffer B; 290–390 min, 100% buffer B. Fractions of 10 ml were collected.

Column 2, 16 mm×12 cm Heparin–agarose II-S (Sigma, St Louis, MO) (flow-rate = 2 ml/min). Peak fractions from column 1 were diluted 3:2 with buffer C (10 mM Bis-Tris, pH 6.5 with HCl) and the pH was adjusted to 6.5. After sample loading, the column was eluted with a gradient generated by mixing buffer C with buffer D (buffer C plus 1 M NaCl): 0–30 min, 0% buffer D; 30–110 min, 15–55% buffer D; 110–140 min, 100% buffer D. Fractions of 10 ml were collected.

Column 3, 5 mm×6 cm Green A (Amicon, Beverly, MA) (flow-rate = 0.5 ml/min). $MgSO_4$ (2 mM final) was added to the peak fractions from column 2, which was then diluted 1:1 with buffer E (10 mM Bis-Tris, 2 mM $MgSO_4$, pH 7.2 with HCl). After sample loading, the column was eluted with a gradient generated by mixing buffer E with buffer F (buffer E plus 1 M NaCl): 0–20 min, 0% buffer F; 20–70 min, 25–75% buffer F; 70–90 min, 100% buffer F. Fractions of 2 ml were collected.

Column 4, 16 mm×50 cm Cellufine GCL-90 (Amicon, Beverly, MA) (flow-rate = 0.25 ml/min). Peak fractions from column 3 were loaded, and then eluted with 200 mM NaCl, 10 mM Bis-Tris (pH 7.2 with HCl). Fractions of 5 ml were collected.

Column 5, 5 mm×5 cm Blue A (Amicon, Beverly, MA) (flow-rate = 0.5 ml/min). $MgSO_4$ (2 mM final) was added to the peak fractions. After sample loading, the column was eluted with a gradient generated by mixing buffer E with buffer F: 0–10 min, 0% buffer F; 10–20 min, 20% buffer F; 20–80 min, 20–100% buffer F; 80–100 min, 100% buffer F. Fractions of 2 ml were collected. When these final preparations were supplemented with 2 mg/ml BSA and stored frozen at –20°C, activity declined by ~25% over a 7 day period.

Protein concentration was determined either as described previously (Bradford, 1976) or by using a CBQCA protein quantification kit (minimum sensitivity is 10 ng, Molecular Probes, Eugene, OR).

Microsequencing

Multiple preparations of DIPP were pooled for sequencing (~4 μg was used to generate the sequence shown in Figure 2A). DIPP was applied to a Hewlett-Packard hydrophobic sequencing column according to the manufacturer's protocol. *In situ* proteolytic digestion with endoproteinase Lys-C was performed as previously described (Burkhart, 1993). Peptides were separated on RP-HPLC (Burkhart, 1993) using a Hypersil C-18 column (0.8×250 mm, LC Packings). *In situ* cyanogen bromide (CNBr) cleavage was performed on the HP1004A Protein Chemistry Station according to the HP methods. Briefly, 2 mg of CNBr in 400 μl of 70% formic acid was placed in the column reservoir. After passing ~300 μl of the CNBr/acid solution through the column, the column was left at room temperature for 16 h. After washing with 500 μl of water followed by 500 μl of 0.1 M Tris–HCl pH 8.5, the CNBr fragments were batch eluted from the column using 500 μl of 80% acetonitrile. The eluted peptides were dried under vacuum and resuspended in SDS loading buffer. The CNBr fragments were electrophoresed using a 16% Novex mini-gel (100×100×1 mm) in Tris-tricine buffer. Peptides were then electroblotted onto Trans-Blot PVDF, stained and excised for sequencing. All automated sequencing was performed on the HP G1005A Protein Sequencing System.

Molecular cloning, expression and purification of DIPP

The dbEST cDNA clone with IMAGE clone ID # 486790 (DDBJ/EMBL/GenBank accession No. AA043224) was obtained from the ATCC. Plasmid DNA was prepared using a Qiagen kit, and the insert DNA was sequenced completely using a PCR-based rhodamine fluorescent dye method (Perkin-Elmer). Sequence reactions were analyzed using an ABI 377 sequencer and related software. The sequence of this human uterine 1222 bp DIPP clone has been deposited with the DDBJ/EMBL/GenBank accession No. AF062529. [A second, independent dbEST cDNA clone (IMAGE ID # 469920, DDBJ/EMBL/GenBank accession No. AA029904) from the same tissue source was also sequenced, and was found to contain a 1091 bp insert, the initial 1070 bp of which were identical to the 1222 bp DIPP cDNA; this has been deposited with GenBank accession No. AF062530.] A 5′ primer identical to nucleotides 160–183 and a 3′ primer identical to the reverse complementary sequence from nucleotide 662 to 689 of the 1222 bp clone were used in PCRs containing P*fu* DNA polymerase (Stratagene) to amplify the coding sequence of DIPP. The 5′ and 3′ primers contained a *Bam*HI site and a *Sal*I site, respectively. The resulting 530 bp PCR product was cloned into the *Bam*HI and *Sal*I sites of pQE30 (Qiagen), and completely sequenced as described above to confirm the structure of the construct ($pHis_6$-DIPP). This cloning scheme creates a recombinant protein which contains the $MRGSH_6GS$ sequence immediately upstream of Lys-3 of DIPP.

To express recombinant protein, *E.coli* (strain M15) were transformed with either $pHis_6$-DIPP or pQE-30 and cultured until A_{600} 0.8. Following induction with 1 mM isopropyl-β-D-thiogalactopyranoside (IPTG) for 6 h at 37°C, cells were harvested and incubated for 1 h in 5 vols of buffer G (300 mM NaCl, 20 mM Tris, pH 8.0 with HCl), supplemented with 5 μg/ml leupeptin, 1 μg/ml aprotinin and 1 mg/ml lysosyme. Following three rapid freeze–thaw cycles, particulate matter was removed by centrifugation. The supernatant was applied to (and subsequently eluted from) a 5 mm×5 cm Ni-NTA Superflow column (Qiagen) at a flow-rate of 1 ml/min. The column was washed for 12 min with buffer G. Bound protein was eluted with a gradient generated by mixing buffer G with buffer H (buffer G plus 0.5 M imidazole) as follows: 0–20 min, 0–50% buffer H; 20–30 min, 100% buffer H. Fractions containing DIPP were stored at –20°C.

Preparation of E70Q DIPP mutant

An E70Q DIPP mutant was prepared by using the QuickChange™ Site-Directed Mutagenesis Kit (Stratagene), according to the manufacturer's instructions. Two complementary mutagenic primers (5′-GTC TGT GAG CAG GCT GGA G-3′ for the sense strand), containing one base mismatch (underlined) in the codon for Glu70, were synthesized with a Beckman Oligo 1000M DNA Synthesizer. $pHis_6$-DIPP was used as template for PCR using the mutagenic primers. The wild-type strand in the resulting PCR product was removed by digestion with 10 U of *Dpn*I at 37°C for 1 h before being used to transform *E.coli* XL1-Blue supercompetent cells. The colonies from the transformation plates were screened by colony PCR with two primers flanking the DIPP gene, and plasmids were prepared from the colonies that generated the expected PCR product. After confirming the DNA sequence of the E70Q DIPP, the mutant cDNA was transformed into M15-competent cells for protein expression, as described above.

Northern blots

A 430 bp, digoxigenin-labeled dsDNA probe was generated with a PCR probe-labeling kit (Boehringer Mannheim) according to the manufacturer's instructions, using primers which amplified most of the DIPP-coding sequence. The probe (200 ng/ml DIG Easy Hyb solution) was incubated with a multiple tissue Northern blot (Clontech) at 50°C overnight. The blot was washed twice at room temperature with 2× SSC/0.1% SDS for 5 min each, followed by two washes in 0.1× SSC/0.1% SDS for 15 min each at 65°C. The washed blot was processed for chemiluminescent detection of bound probe using an alkaline phosphatase-conjugated anti-digoxigenin antibody and CDP-STAR according to the manufacturer's protocol (Boehringer Mannheim), followed by autoradiography using Kodak BioMax X-ray film. The blot was then stripped by washing in 0.25% (w/v) SDS heated to 95°C for 10 min. β-actin was detected in a similar manner using a 455 bp digoxigenin-labeled β-actin dsDNA probe.

Additional materials

All samples of PP-$InsP_5$ and $[PP]_2$-$InsP_4$ (either non-radiolabeled, ^{32}P-labeled or ^3H-labeled) were synthesized by M.E.Bembenek at NEN. PP-$[^3H]InsP_4$ and $[^3H]InsP_5$ were prepared as previously described (Menniti *et al.*, 1993). $[^3H]InsP_6$ was purchased from NEN. Non-radiolabled $InsP_6$ was purchased from Calbiochem, while inorganic pyrophosphatase, dAMP, dADP, dATP and Ins(1,3,4,5,6)P_5 were purchased from Sigma, and both Ins(1,4,5)P_3 and Ins(1,3,4,5)P_4 were purchased from the Rhode Island Foundation. $[^3H]$dATP was purchased from ICN Pharmaceuticals Inc. (Costa Mesa, CA).

Acknowledgements

We are grateful to our colleagues Drs J.W.Putney,Jr, J.Cidlowski and R.Schaaper for their helpful comments on the manuscript.

References

Albert,C., Safrany,S.T., Bembenek,M.E., Reddy,K.M., Reddy,K.K., Falck,J.R., Bröker,M., Shears,S.B. and Mayr,G.W. (1997) Biological variability in the structures of diphosphoinositol polyphosphates in *Dictyostelium discoideum* and mammalian cells. *Biochem. J.*, **327**, 553–560.

Ali,N., Duden,R., Bembenek,M.E. and Shears,S.B. (1995) The interaction of coatomer with inositol polyphosphates is conserved in *Saccharomyces cerevisiae*. *Biochem. J.*, **310**, 279–284.

Bessman,M.J., Frick,D.N. and O'Handley,S.F. (1996) The MutT proteins or 'Nudix' hydrolases, a family of versatile, widely distributed, 'housecleaning' enzymes. *J. Biol. Chem.*, **271**, 25059–25062.

Bhatnagar,S.K., Bullions,L.C. and Bessman,M.J. (1991) Characterization of the *mut*T nucleoside triphosphatase of *Escherichia coli*. *J. Biol. Chem.*, **266**, 9050–9054.

Bradford,M.M. (1976) A rapid and sensitive method for the quantitation of microgram quantities of protein utilizing the principle of protein–dye binding. *Anal. Biochem.*, **72**, 248–254.

Brearley,C.A. and Hanke,D.E. (1996) Inositol phosphates in barley (*Hordeum vulgare L.*) aleurone tissue are stereochemically similar to the products of breakdown of $InsP_6$ *in vitro* by wheat-bran phytase. *Biochem. J.*, **318**, 279–286.

Bullions,L.C., Méjean,V., Claverys,J.-P. and Bessman,M.J. (1994) Purification of the MutX protein of *Streptococcus pneumoniae*, a homologue of *Escherichia coli* MutT. Identification of a novel catalytic domain for nucleoside triphosphate pyrophosphohydrolase activity. *J. Biol. Chem.*, **269**, 12339–12344.

Burkhart,W. (1993) *In situ* proteolytic digestions performed on proteins bound to the Hewlett-Packard hydrophobic sequencing column. In Angeletti,R. (ed.), *Techniques in Protein Chemistry IV.* Academic Press, New York, NY, pp. 399–406.

Craxton,A., Caffrey,J.J., Burkhart,W., Safrany,S.T. and Shears,S.B. (1997) Cloning and expression of rat hepatic multiple inositol polyphosphate phosphatase. *Biochem. J.*, **328**, 75–81.

French,P.J., Bunce,C.M., Stephens,L.R., Lord,J.M., McConnell,F.M., Brown,G., Creba,J.A. and Michell,R.H. (1991) Changes in the levels of inositol lipids and phosphates during the differentiation of HL60 promyelocytic cells towards neutrophils or monocytes. *Philos. Trans. R. Soc. Lond. (Biol.)*, **245**, 193–201.

Ganzhorn,A.J. and Chanal,M.-C. (1990) Kinetic studies with myo-inositol monophosphatase from bovine brain. *Biochemistry*, **29**, 6065–6071.

Glennon,M.C. and Shears,S.B. (1993) Turnover of inositol pentakisphosphates, inositol hexakisphosphate and diphosphoinositol polyphosphates in primary cultured hepatocytes. *Biochem. J.*, **293**, 583–590.

Hoenig,M., Lee,R.J. and Ferguson,D.C. (1989) A microtiter plate assay for inorganic phosphate. *J. Biochem. Biophys Methods*, **19**, 249–252.

Jackson,I.J. (1991) A reappraisal of non-consensus mRNA splice sites. *Nucleic Acids Res.*, **19**, 3795–3798.

Kisselev,L.L., Justesen,J., Wolfson,A.D. and Frolova,L.Y. (1998) Diadenosine oligophosphates (ApnA), a novel class of signalling molecules? *FEBS Lett.*, **427**, 157–163.

Kozak,M. (1996) Interpreting cDNA sequences: some insights from studies on translation. *Mamm. Genome*, **7**, 563–574.

Lin,J., Abeygunawardana,C., Frick,D.N., Bessman,M.J. and Mildvan, A.S. (1996) The role of Glu 57 in the mechanism of the *Escherichia coli* MutT enzyme by mutagenesis and heteronuclear NMR. *Biochemistry*, **35**, 6715–6726.

Lin,J., Abeygunawardana,C., Frick,D.N., Bessman,M.J. and Mildvan, A.S. (1997) Solution structure of the quarternary MutT–M^{2+}–AMPCPP–M^{2+} complex and mechanism of its pyrophosphorylase action. *Biochemistry*, **36**, 1199–1211.

Liu,X., Kim,C.N., Yang,J., Jemmerson,R. and Wang,X. (1996) Induction of apoptotic program in cell-free extracts: requirement for dATP and cytochrome *c*. *Cell*, **86**, 147–157.

Martin,J.B., Bakker-Grunwald,T. and Klein,G. (1993) ^{31}P-NMR analysis of *Entomoeba histolytica.* Occurrence of high amounts of two inositol phosphates. *Eur. J. Biochem.*, **214**, 711–718.

Martin,J.-B., Bakker-Grunwald,T. and Klein,G. (1995) Metabolites of the free-living amoeba *Phreatamoeba balamuthi* analyzed by ^{13}C- and ^{31}P-NMR spectroscopy: occurrence of phosphoinositol diphosphates. *J. Euk. Microbiol.*, **42**, 183–191.

Menniti,F.S., Miller,R.N., Putney,J.W.,Jr and Shears,S.B. (1993) Turnover of inositol polyphosphate pyrophosphates in pancreatoma cells. *J. Biol. Chem.*, **268**, 3850–3856.

Mo,J.-Y., Maki,H. and Sekiguchi,M. (1992) Hydrolytic elimination of a mutagenic nucleotide, 8-oxodGTP, by human 18-kilodalton protein: sanitization of nucleotide pool. *Proc. Natl Acad. Sci. USA*, **89**, 11021–11025.

O'Handley,S.F., Frick,D.N., Bullions,L.C., Mildvan,A.S. and Bessman, M.J. (1996) *Escherichia coli* orf17 codes for a nucleoside triphosphate pyrophosphatase member of the mutT family of proteins. Cloning, purification and characterization of the enzyme. *J. Biol. Chem.*, **271**, 24649–24654.

O'Handley,S.F., Frick,D.N., Dunn,C.A. and Bessman,M.J. (1998) Orf186 represents a new member of the nudix hydrolases, active on adenosine (5′)triphospho (5′)adenosine, ADP-ribose and NADH. *J. Biol. Chem.*, **273**, 3192–3197.

Putney,J.W.,Jr (1991) Capacitative calcium entry revisited. *Cell Calcium*, **11**, 611–624.

Romano,P., Wang,J., O'Keefe,R.J., Puzas,J.E., Rosier,R.N. and Reynolds,P.R. (1998) HiPER1, a phosphatase of the endoplasmic reticulum with a role in chondrocyte maturation. *J. Cell Sci.*, **111**, 803–813.

Safrany,S.T. and Shears,S.B. (1998) Turnover of bis-diphosphoinositol tetrakisphosphate in a smooth muscle cell line is regulated by β_2-adrenergic receptors through a cAMP-mediated, A-kinase- independent mechanism. *EMBO J.*, **17**, 1710–1716.

Shears,S.B. (1992) Metabolism of inositol phosphates. In Putney,J.W.,Jr (ed.), *Advances in Second Messenger and Phosphoprotein Research*. Raven Press, New York, NY, pp. 63–92.

Shears,S.B., Ali,N., Craxton,A. and Bembenek,M.E. (1995) Synthesis and metabolism of *bis*-diphosphoinositol tetrakisphosphate *in vitro* and *in vivo. J. Biol. Chem.*, **270**, 10489–10497.

Singh,J., Hunt,P., Eggo,M.C., Sheppard,M.C., Kirk,C.J. and Michell,R.H. (1996) Thyroid-stimulating hormone rapidly stimulates inositol polyphosphate formation in FRTL-5 thyrocytes without activating phosphoinositidase C. *Biochem. J.*, **316**, 175–182.

Stephens,L.R., Radenberg,T., Thiel,U., Vogel,G., Khoo,K.-H., Dell,A., Jackson,T.R., Hawkins,P.T. and Mayr,G.W. (1993) The detection, purification, structural characterization and metabolism of diphosphoinositol pentakisphosphate(s) and bisdiphosphoinositol tetrakisphosphate(s). *J. Biol. Chem.*, **268**, 4009–4015.

Szwergold,B.S., Graham,R.A. and Brown,T.R. (1987) Observation of inositol pentakis- and hexakis-phosphates in mammalian tissues by ^{31}P NMR. *Biochem. Biophys. Res. Commun.*, **149**, 874–881.

Thorne,N.M.H., Hankin,S., Wilkinson,M.C., Nuñez,C., Barraclough,R. and McLennan,A.G. (1995) Human diadenosine 5′,5″-P1,P4-tetraphosphate pyrophosphorylase is a member of the MutT family of nucleoside pyrophosphatases. *Biochem. J.*, **311**, 717–721.

Voglmaier,S.M., Bembenek,M.E., Kaplin,A.I., Dormán,G., Olszewski, J.D., Prestwich,G.D. and Snyder,S.H. (1996) Purified inositol hexakisphosphate kinase is an ATP synthase: diphosphoinositol pentakisphosphate as a high-energy phosphate donor. *Proc. Natl Acad. Sci. USA*, **93**, 4305–4310.

Voglmaier,S.M., Bembenek,M.E., Kaplin,A.I., Dormán,G., Olszewski, J.D., Prestwich,G.D. and Snyder,S.H. (1997) Purification and assay of inositol hexakisphosphate kinase and diphosphoinositol pentakisphosphate kinase. In Shears,S.B. (ed.), *Signalling by Inositides: A Practical Approach*. IRL Press at Oxford University Press, Oxford, UK, pp. 195–201.

Received May 22, 1998; revised August 13, 1998; accepted September 18, 1998